# Nonlocal orbital-free noninteracting free-energy functional for warm dense matter

Travis Sjostrom and Jérôme Daligault
*Theoretical Division, Los Alamos National Laboratory, Los Alamos, New Mexico 87545, USA*
(Received 23 August 2013; published 4 November 2013)

We have extended nonlocal orbital-free methods which enforce the correct linear response in the noninteracting uniform electron gas limit, developed at zero temperature for the kinetic energy to finite temperature for the full noninteracting free energy. Comparisons are made to the Thomas-Fermi approximation and to the orbital-dependent Kohn-Sham method. We find significantly improved agreement for the resulting functional with Kohn-Sham for a wide range of densities and temperatures. We also provide the necessary formulas for implementation in quantum molecular dynamics simulations.

DOI: 10.1103/PhysRevB.88.195103 PACS number(s): 71.15.Mb, 71.10.−w, 71.15.Pd

## I. INTRODUCTION

Warm dense systems present significant challenges for *ab initio* simulations. In order to incorporate the quantum nature of these systems, state-of-the-art approaches use Kohn-Sham density functional theory (DFT). The number of orbitals required in this approach, however, scales with the temperature, making it computationally prohibitive. In recent years attention has been given to finite temperature orbital-free (OF) DFT, which depends only on the density and does not suffer the same scaling issue. For the most part the finite temperature Thomas-Fermi approximation has been used.[1,2] Some efforts[3] have made use of the gradient (Wigner-Kirkwood) expansion.[4,5] More recently, a generalized gradient form has been investigated.[6] Interestingly, for systems from simple metals and semiconductors to molecules, zero temperature OF DFT efforts have made use of nonlocal functionals based upon correcting the response of the kinetic energy functional, with marked improvement of system properties including total energy and lattice constants, over gradient methods for the kinetic energy.[7–14] Here we extend this approach to the noninteracting free energy of finite temperature systems.

For finite temperature we may write the total free energy as a functional of the density alone as follows:[15]

$$F[n,T] = F_s[n,T] + F_H[n] + F_{xc}[n,T] + F_{ei}[n] + F_{ii}, \tag{1}$$

where $F_s$ is the noninteracting free energy comprised of both kinetic and entropic parts, $F_H$ is the Hartree energy or direct Coulomb interaction between the electrons, $F_{ei}$ and $F_{ii}$ are the electron-ion and ion-ion Coulomb interactions, respectively, and $F_{xc}$ is defined as the remainder of the total free energy, which includes the quantum mechanical exchange and correlation as well as the excess kinetic and entropic terms.

Of the terms given in Eq. (1), only $F_s$ and $F_{xc}$ lack explicit calculable forms and hence require approximate forms in OF DFT. The Kohn-Sham method alleviates the need for an approximate $F_s$ by introduction of a fictitious system of noninteracting particles which, while remarkably successful, scales as the number of orbitals cubed. This scaling limits system size, by electron number, at zero temperature and limits accessible temperatures due to the increase of fractionally occupied orbitals included in the calculation with temperature increase. While computationally massive Kohn-Sham calculations have been performed probing into the warm dense matter regime,[16,17] OF DFT could offer accessibility to much higher temperatures at a fraction of the computational cost, provided we have a good approximations for $F_s$ and $F_{xc}$. Finite temperature $F_{xc}$ has recently been examined for the local density approximation.[18] In this work we focus on an $F_s$ functional to achieve results of Kohn-Sham accuracy in regions far beyond the applicable range of the Thomas-Fermi approximation.

The remainder of the paper will first offer the definition and construction of this functional; then we present results for some simple systems in comparison with other OF functionals as well as Kohn-Sham methods. Additionally, in Appendix B we provide necessary quantities for implementation of the functional in quantum molecular dynamics simulations.

## II. RESPONSE CORRECTED FREE-ENERGY FUNCTIONALS

To improve upon current free-energy functionals we consider a basic property of an electron system, the density-density response function $\chi(\mathbf{r},\mathbf{r}',T,n_0)$, which for the homogeneous systems of interest is a function of $\mathbf{r}-\mathbf{r}'$ only. For a given approximate noninteracting free energy $F_S$, the corresponding density-density response function for the uniform electron gas is

$$\chi(\mathbf{r}-\mathbf{r}',T,n_0) = -\left(\left.\frac{\delta^2 F_s[n,T]}{\delta n(\mathbf{r})\delta n(\mathbf{r}')}\right|_{n_0}\right)^{-1}, \tag{2}$$

where $T$ and $n_0$ are the electron gas temperature and density, respectively. The exact response is given by the Lindhard function (Appendix A). Popular approximations for $F_s$ do not reproduce the Lindhard function. Our goal is to construct a functional that reproduces this exact result.

To illustrate the failure of local (and semilocal) functionals for this response condition and motivate the form of the proposed functional, we extend previous considerations at zero $T$.[19,20] In Fig. 1 we plot the Fourier transform $\tilde{\chi}(q,T,n_0)$ of the response result of Eq. (2) for the uniform electron gas at $T = 50.1$ eV and reduced density $r_s = 1$, where $r_s = (3/4\pi n)^{1/3}/a_B$. First, for reference, the exact Lindhard result is shown. Second, the Thomas-Fermi approximation (TF) is shown [see Eq. (4)]; it has no $q$ dependence and is correct only at $q = 0$. Third, the gradient-dependent von Weizsäcker

 

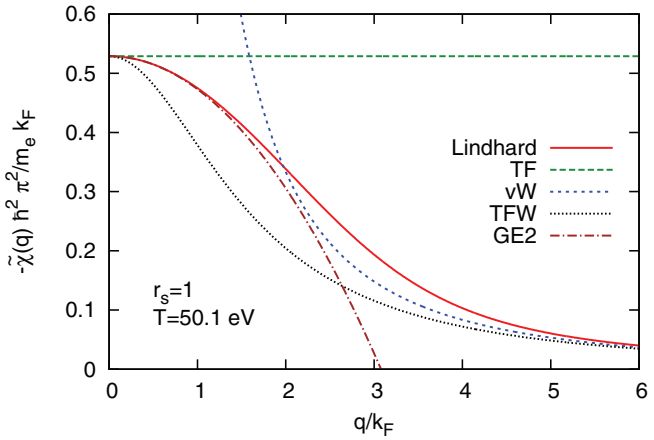


FIG. 1. (Color online) Response function of several local free-energy functionals compared with the exact Lindhard result for the uniform electron gas, $k_F = (3\pi^2 n_0)^{1/3}$.

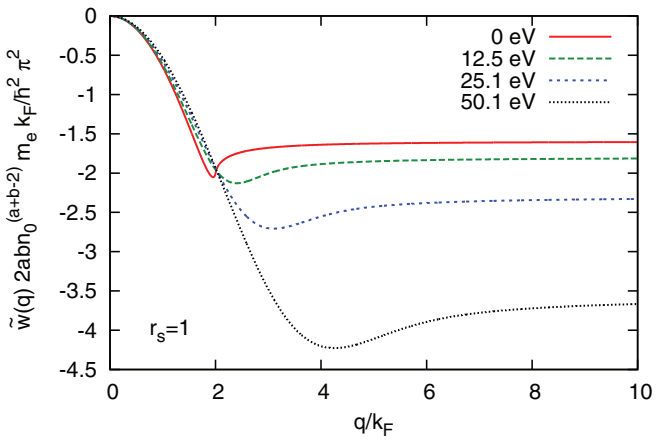


FIG. 2. (Color online) The kernel $\tilde{w}_{a,b}$ with $a = b = 5/6$ for electron density $r_s = 1$ and several different temperatures given in electronvolts.

term (vW) is shown [see Eq. (5)]; this is correct in the large $q$ limit but diverges for small $q$. The sum of the previous two terms gives the Thomas-Fermi-Weizsäcker (TFW) functional, which has the advantage of being correct at $q = 0$ and in the large $q$ limit, but fails at intermediate $q$. Finally we show the gradient expansion of TF to second order (GE2), as given by Perrot,[4] which enforces the correct response for small $q$ to second order. Though fourth-order TF gradient expansion further improves the results, it still does not go to the correct limit and divergence problems for real densities begin at sixth order.[21,22]

It is clear that TF, vW, and linear combinations cannot reproduce the exact response. A nonlocal functional, however, may be used to achieve this. Following the zero-temperature formalism, we separate the functional into a sum of TF, vW, and a nonlocal term. This separation is well motivated by Fig. 1, as the nonlocal contribution $F_{a,b}$ can be seen as an interpolative correction between the large and small $q$ limits which are satisfied by a functional simply summing TF and vW,

$$F_s[n,T] = F_{TF}[n,T] + F_{vW}[n] + F_{a,b}[n,T]\ . \tag{3}$$

The first term on the right-hand side is the finite temperature Thomas-Fermi term, which is correct in the high-temperature limit,

$$F_{TF}[n,T] = \int f_{TF}[n(\mathbf{r}),T]\ d\mathbf{r}\ , \tag{4}$$

where $f_{TF}$ is just the noninteracting electron gas energy per volume. Second is the von Weizsäcker term, which is exact for the single-orbital system and also is a lower bound to the finite temperature kinetic energy,

$$F_{vW}[n] = \frac{\hbar^2}{m_e}\int \frac{|\nabla n(\mathbf{r})|^2}{8n(\mathbf{r})}\ d\mathbf{r}\ . \tag{5}$$

For the final term we choose the finite temperature extension of the nonlocal zero $T$ form originally given by Wang and Teter,[7]

$$F_{a,b}[n,T] = \iint n^a(\mathbf{r}) w_{a,b}(\mathbf{r}-\mathbf{r}',T) n^b(\mathbf{r}')\ d\mathbf{r}\ d\mathbf{r}'\ . \tag{6}$$

Here the powers $a$ and $b$ and the kernel $w$ are to be determined. Recall that the purpose is to enforce the correct linear response for the uniform electron gas. This is done by evaluating the response of Eq. (3) according to Eq. (2) and setting the result equal to the exact (Lindhard) response $\chi_0$. Then in the Fourier transform we have

$$\tilde{\chi}_{TF}^{-1}(T,n_0) + \tilde{\chi}_{vW}^{-1}(q,T,n_0) + \tilde{\chi}_{a,b}^{-1}(q,T,n_0) \equiv \tilde{\chi}_0^{-1}(q,T,n_0), \tag{7}$$

with all terms of the above equation given in Appendices A and B. Finally, subject to the condition that $\tilde{w}_{a,b}(q=0,T,n_0) = 0$, we can solve Eq. (7) for the kernel,

$$\tilde{w}_{a,b}(q,T,n_0) = \frac{-\tilde{\chi}_0^{-1} + \tilde{\chi}_{TF}^{-1} + \tilde{\chi}_{vW}^{-1}}{2abn_0^{(a+b-2)}}\ , \tag{8}$$

where we have dropped the dependencies on the right-hand side for clarity.

This leaves now the determination of $a$ and $b$. Various values have been used at zero $T$. Nonempirical determination can be made by examining small variations from the uniform electron gas in both the large and small $q$ limits.[10] A judicious choice that does well in both the large and small $q$ limits is the original parameters of Wang and Teter, $a = b = 5/6$, which we will employ throughout the remainder of this work and hence label our total free-energy functional

$$F_{WT} = F_{TF} + F_{vW} + F_{5/6,5/6}\ . \tag{9}$$

We note also that up to this point $a$ and $b$ have been arbitrary. Nonequal values as well as temperature-dependent values might be explored.

For illustration of the temperature dependence, the kernel is plotted in Fig. 2 for reduced density $r_s = 1$ at several different temperatures, and with $a = b = 5/6$.

## III. RESULTS AND COMPARISONS

We have implemented the nonlocal free-energy functional Eq. (9) for periodic systems through modification of the zero $T$ OF DFT code PROFESS.[23] As a preliminary calculation we have

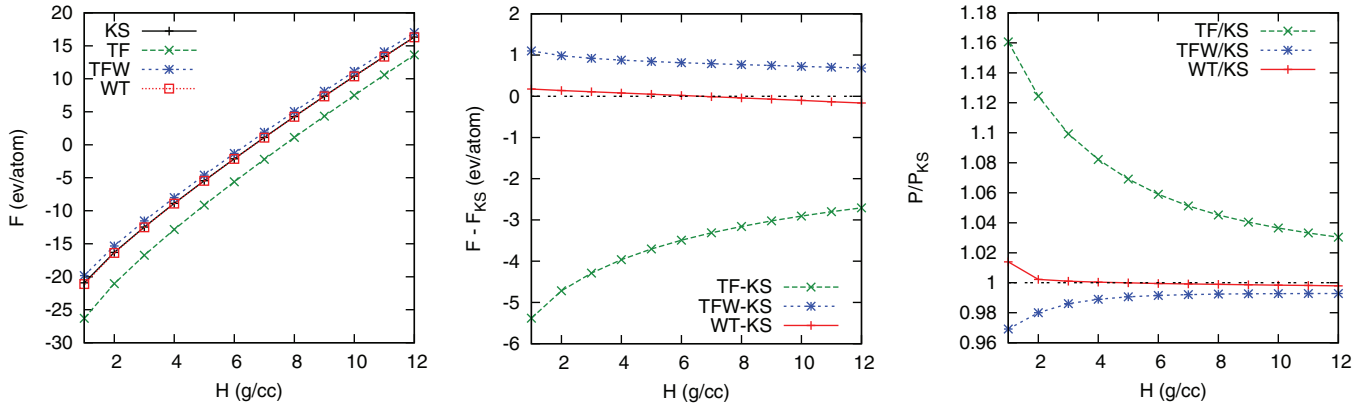


FIG. 3. (Color online) Simple cubic hydrogen at temperature 100 000 K (8.617 eV) is shown for densities from 1 to 12 g/cc. From left to right is shown the free energy per atom, the difference of the free energy per atom of the OF methods with that of KS, and the ratio of the pressures of the OF methods with the KS pressure. This nonlocal functional shows a very significant improvement over the Thomas-Fermi and Thomas-Fermi plus von Weizsäcker functionals.

considered a fixed geometry system, simple cubic hydrogen (sc H), at a wide range of temperatures and densities. In addition to the functional $F_{WT}$, labeled in all figures as WT, we compare with the Thomas-Fermi approximation TF, and the Thomas-Fermi plus full von Weizsäcker, TFW. The last is given by the first two terms on the right-hand

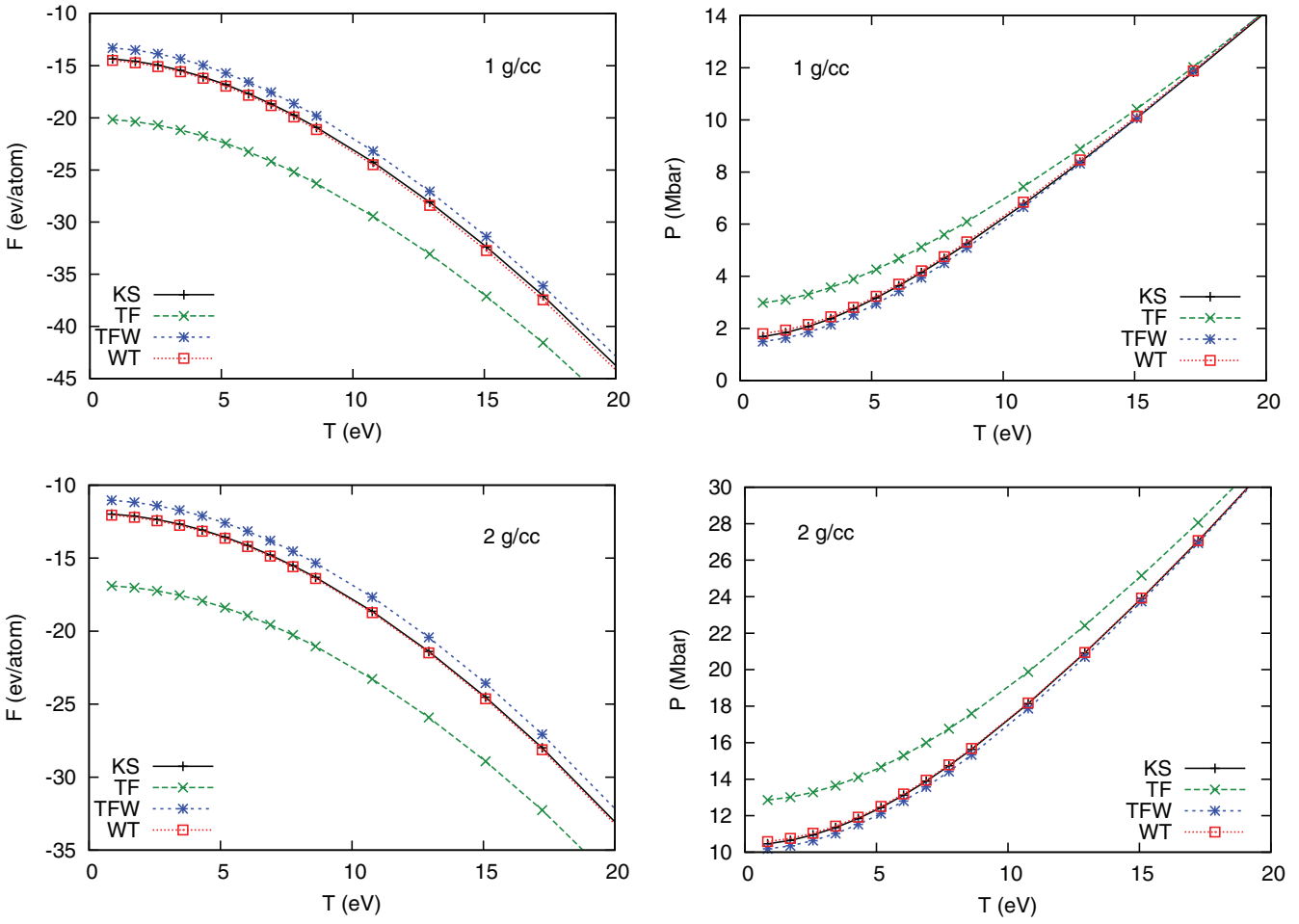


FIG. 4. (Color online) Simple cubic hydrogen at fixed densities, 1 g/cc (top panels) and 2 g/cc (bottom panels) as a function of temperature from 10 000–200 000 K (0.861 7–17.23 eV). Free energy is shown in the left panels for several OF and KS DFT calculations, and pressure is shown on the right. Very good agreement for the functional with respect to KS is seen, as well as significant improvement of the Thomas-Fermi approximation.

side of Eq. (3) and not to be confused with the gradient expansion of Perrot,[4] which has a reduced von Weizsäcker term. The pseudopotential for the OF DFT calculations has been generated by the Goodwin-Needs-Heine method, as described in Ref. 6, with cutoff radius $r_c = 0.25$ bohr. All calculations were performed with a $64 \times 64 \times 64$ reciprocal grid containing 216 atoms.

In addition to the OF DFT results, we also calculate as a benchmark the same systems in Kohn-Sham (KS) DFT. Here we use the plane-wave code QUANTUM-ESPRESSO,[24] with a small cutoff radius, $r_c = 0.45$ bohr, pseudopotential of the projector-augmented-wave variety, valid for warm-dense-matter conditions.[6] The KS calculations were performed for a single-atom cell, where the plane-wave energy cutoff was set at 200 Ry and the $k$ grid for Brillouin zone integration was at minimum $17 \times 17 \times 17$. The number of bands varied with temperature such that a threshold of $10^{-6}$ was achieved for the thermal occupation numbers. For example, at 10 000, 100 000, and 200 000 K, the number of bands required were 2, 8, and 16 at 1 g/cc and 2, 4, and 8 at 2 g/cc. In the reduced Brillouin zone scheme for a $17 \times 17 \times 17$ $k$ grid, there were 2457 unique $k$ points, making the number of orbitals in the calculation 2457 times the number of bands. Both the OF and KS DFT use the Perdew-Zunger local density approximation for the exchange-correlation energy.[25]

We note here that the local pseudopotential provides a regularization of the Coulomb potential inside of the cutoff radius, without which much finer numeric grids would be required to achieve accurate results. The nonlocal pseudopotentials used in KS DFT provide, as well, this type of regularization near the nucleus but also allow for different potentials for different angular momentum states and allow exclusion of core electrons from the calculation for higher Z elements.

The pressure and free energy results, exclusive of any ion kinetic contributions, for the sc H system are shown in Figs. 3 and 4. In the first set (Fig. 3), the sc H system is at constant temperature $T = 100\ 000$ K (8.617 eV) and the lattice is compressed from 1 to 12 g/cc. In the leftmost panel the free energy per atom for each of the three OF methods and KS are shown. While TFW shows a great improvement over TF, the KS crosses lie nearly centered in the boxes marking WT for all densities shown. In the middle panel, the differences of the OF methods with KS are shown along with the zero line for reference. Though there is slope in the WT line, it remains very close to zero. The last panel shows the pressure of the OF results relative to KS; again, a significant improvement is seen with WT.

In Fig. 4 the free energy per atom and the pressure for the sc H system are shown at 1 (top) and 2 (bottom) g/cc as a function of the temperature. Similar trends as before are seen, including good agreement between WT and KS, where KS calculations are performed from 10 000 to 200 000 K.

Briefly we discuss two functionals not shown yet. First is the second-order gradient expansion GE2 given by Perrot[4] and the second is the generalized gradient approximation (GGA) given in Ref. 6, in which both of those functionals are examined in more detail. The GE2 does improve moderately upon TF, while the GGA actually produces results that lie close to the TFW presented here. Figure 5 shows these two functionals in comparison to the functionals shown in Fig. 4.

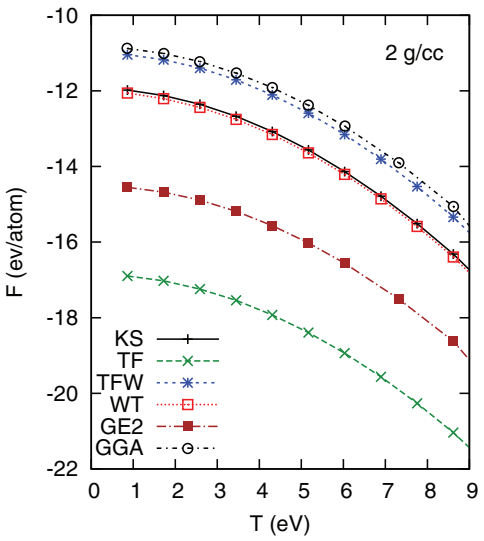


FIG. 5. (Color online) Simple cubic hydrogen free energy per atom at 2 g/cc as a function of temperature from 10 000 to 100 000 K (0.861 7–8.617 eV) for several OF functionals and KS DFT.

## IV. CONCLUSIONS

We have extended and implemented a nonlocal orbital-free free-energy functional enforcing the correct linear response for the uniform electron gas at finite temperature. By construction this nonlocal functional should be most applicable for free-electron-like systems; this is the same argument that can be made for Thomas-Fermi or Thomas-Fermi plus the gradient expansion. However, the addition of the full von Weizsäcker term greatly improves results for nonuniform systems beyond the last two mentioned methods, due to the correctness of the large $q$ limit of the response. Adding then the interpolative nonlocal term further increases the accuracy for nonuniform systems even quite distant from the free-electron-like system.

Our implementation using the Wang-Teter parameters for $a$ and $b$ have shown excellent agreement with Kohn-Sham, far beyond Thomas-Fermi, Thomas-Fermi plus gradient expansion, and Thomas-Fermi plus full von Weizsäcker. Importantly, this greatly extends the regime where OF DFT results can be used as opposed to computationally expensive, even prohibitive Kohn-Sham calculations. Though there is increased cost with the nonlocal functional, it still scales as local methods due to the efficient reciprocal space implementation. In particular, we have seen only a couple to a few times the computation time between Thomas-Fermi and Wang-Teter. In general, these orbital-free methods scale only with the physical size of the unit cell, as a larger cell requires more grid points to achieve the same accuracy. There is no scaling with temperature as there is in KS DFT due to the increase of fractionally occupied orbitals.

The kernel of our functional depends only on the average density, not the local density; hence it is a density-independent kernel, and it is constructing to reproduce the density-density response. In the zero-$T$ literature there exist nonlocal functionals which make use of a density-dependent kernel or are constructed to enforce higher-order response terms. These methods can improve accuracy but in general will increase the computational cost dramatically. Hence

the density-independent kernel presented here provides a computationally effective bridge between Kohn-Sham and Thomas-Fermi calculations for accurate characterization of warm dense systems.


## ACKNOWLEDGMENTS

This research was supported by the DOE Office of Fusion Sciences (FES), and by the NNSA of the US DOE at Los Alamos National Laboratory under Contract No. DE-AC52-06NA25396. We also would like to thank Dr. Valentin Karasiev for providing the GE2 and GGA data.


## APPENDIX A: FINITE TEMPERATURE LINDHARD FUNCTION

The finite temperature static Lindhard function for the non-spin-polarized system is given by

$$\tilde{\chi}_0(\mathbf{q},T,n_0) = \frac{2}{(2\pi)^3}\int \frac{f_{\mathbf{k}} - f_{\mathbf{k}+\mathbf{q}}}{\varepsilon_{\mathbf{k}} - \varepsilon_{\mathbf{k}+\mathbf{q}}}\, d\mathbf{k}, \tag{A1}$$

where $f_k = 1/\{\exp[\beta(\varepsilon_k - \mu)] + 1\}$ are the Fermi-Dirac thermal occupations, and $\varepsilon_k = (\hbar k)^2/2m_e$ the single-particle energies. It may be calculated by a one-dimensional integral of the zero temperature Lindhard function as[26]

$$\tilde{\chi}_0(q,T,n_0) = \int_0^\infty dE\, \frac{\tilde{\chi}_0(q,T=0)|_{\varepsilon_F=E}}{4k_BT\cosh^2\left(\frac{E-\mu(T)}{2k_BT}\right)}\,. \tag{A2}$$

It is helpful to have asymptotic expansions available for the Lindhard function, in our case, particularly for large $q$ since we need $\tilde{w}(q)$ to such values of $q$. For this large $q$ limit it is helpful to first write Eq. (A1) as

$$\tilde{\chi}_0(q,T,n_0) = -\frac{m_e}{\hbar^2}\frac{2}{2\pi^2 q}\int_0^\infty f_k\, k \ln\left|\frac{q+2k}{q-2k}\right| dk. \tag{A3}$$

Then, after expanding for large $q$ we may find

$$\tilde{\chi}_0(q,T,n_0) = -\frac{m_e}{\hbar^2}\frac{k_F}{\pi^2}x^2\left[1 + \sum_{n=1}^{\infty} x^{2n}\frac{3^{n+1}}{2(2n+1)}t^{(n+3/2)}I_{(n+1/2)}(\eta_0)\right], \tag{A4}$$

where $k_F = (3\pi^2 n_0)^{1/3}$, $x^2 = 4k_F^2/3q^2$, $t = 2/\beta k_F^2$, and $I_{1/2}(\eta_0) = (2/3)t^{-3/2}$. The $I_\nu$ functions are all Fermi integrals given by

$$I_\nu(z) = \int_0^\infty \frac{dy\; y^\nu}{e^{y-z}+1}\,, \quad \nu \geqslant -\frac{1}{2}\,. \tag{A5}$$

In the long-wavelength regime, we may expand Eq. (A1) for small $q$ to find

$$\tilde{\chi}_0(q,T,n_0) = -\frac{1}{2\pi^2}\left(\frac{2}{\beta}\right)^{1/2}\left[I_{-1/2}(\eta_0)\left(\frac{m_e}{\hbar^2}\right)^{3/2} - q^2\frac{\beta}{12}\frac{d}{d\eta_0}[I_{-1/2}(\eta_0)]\left(\frac{m_e}{\hbar^2}\right)^{1/2} + O(q^4)\right]. \tag{A6}$$

Finally, note that for $\tilde{\chi}_0$ in the small and large $q$ expansions the leading terms are $\tilde{\chi}_{TF}$ and $\tilde{\chi}_{vW}$, respectively (see Appendix B).

## APPENDIX B: FUNCTIONAL DETAILS FOR MOLECULAR DYNAMICS

Orbital-free DFT requires solution of a single Euler-Lagrange equation $\delta F/\delta n - \mu = 0$. Each free-energy term, as given in Eq. (1), therefore has a corresponding potential given by the functional derivative with respect to $n$. Another consideration is that in molecular dynamics the pressure is calculated by the stress tensor as $P = -\mathrm{Tr}\,\overleftrightarrow{\sigma}/3$, where the stress tensor is given by the derivative with respect to the infinitesimal strain $\sigma_{xx}^{\mu,\nu} = (\partial F_{xx}/\partial\varepsilon_{\mu,\nu})|_{\varepsilon_{\mu,\nu}=0}/\Omega$, where $\Omega$ is the system volume, and $\mu$ and $\nu$ index the coordinates. We now will describe in detail each of the terms of Eq. (3) including their corresponding potentials and stress tensors.

First, for the TF term we provide the free-energy density of Eq. (4):

$$f_{TF}[n(\mathbf{r}),T] = \left(\frac{m_e}{\hbar^2}\right)^{3/2}\frac{\sqrt{2}}{\pi^2\beta^{5/2}} \times\left[-\frac{2}{3}I_{3/2}(\beta\mu_0) + \beta\mu_0 I_{1/2}(\beta\mu_0)\right], \tag{B1}$$

with the electron density given by

$$n(\mathbf{r}) = \left(\frac{m_e}{\hbar^2}\right)^{3/2}\frac{\sqrt{2}}{\pi^2\beta^{3/2}}I_{1/2}(\beta\mu_0)\,, \tag{B2}$$

where the $I_\nu$ are Fermi integrals (see Appendix A). The TF potential is given by the functional derivative, and this is just the noninteracting chemical potential

$$\frac{\delta F_{TF}[n,T]}{\delta n} = \mu_0[n(\mathbf{r})]\,. \tag{B3}$$

In practice, fit functions[6] are used for the elimination of $\mu_0$ from the above equations. The stress tensor is then given by

$$\sigma_{TF}^{\mu,\nu} = \frac{\delta_{\mu,\nu}}{\Omega}\int f_{TF}(n,T) - n\frac{\partial f_{TF}(n,T)}{\partial n}\, d\mathbf{r}\,. \tag{B4}$$

For the vW term the functional derivative and stress tensor are given by

$$\frac{\delta F_{vW}[n]}{\delta n} = \frac{\hbar^2}{m_e}\left(-\frac{1}{4}\frac{\nabla^2 n(\mathbf{r})}{n(\mathbf{r})} + \frac{1}{8}\frac{|\nabla n(\mathbf{r})|^2}{n(\mathbf{r})^2}\right) = -\frac{\hbar^2}{m_e}\frac{1}{2}\frac{\nabla^2 n(\mathbf{r})^{1/2}}{n(\mathbf{r})^{1/2}}\,, \tag{B5}$$

$$\sigma_{vW}^{\mu,\nu} = -\frac{\hbar^2}{m_e}\frac{1}{4\Omega}\int\frac{1}{n(\mathbf{r})}\frac{\partial n(\mathbf{r})}{\partial r_\mu}\frac{\partial n(\mathbf{r})}{\partial r_\nu}\, d\mathbf{r}\,. \tag{B6}$$

Finally, for $F_{a,b}$ the functional derivative may be immediately taken to find

$$\frac{\delta F_{a,b}[n,T]}{\delta n} = an^{a-1}(\mathbf{r})\int w_{a,b}(\mathbf{r}-\mathbf{r}',T)n^b(\mathbf{r}')\, d\mathbf{r}' + bn^{b-1}(\mathbf{r})\int w_{a,b}(\mathbf{r}-\mathbf{r}',T)n^a(\mathbf{r}')\, d\mathbf{r}'\,. \tag{B7}$$

It is convenient for implementation to have the stress tensor in reciprocal space, so first we rewrite the free-energy component

as

$$F_{a,b}[n,T] = \frac{1}{\Omega}\sum_{\mathbf{q}} \tilde{w}_{a,b}(\mathbf{q})\tilde{n}_a(-\mathbf{q})\tilde{n}_b(\mathbf{q}), \tag{B8}$$

where $\tilde{w}_{a,b}(\mathbf{q})$, $\tilde{n}_a(\mathbf{q})$, $\tilde{n}_b(\mathbf{q})$ are the respective Fourier transforms of $w_{a,b}(\mathbf{r}-\mathbf{r}')$, $n^a(\mathbf{r})$, $n^b(\mathbf{r})$. The stress tensor is then given by

$$\begin{aligned}\sigma_{a,b}^{\mu,\nu} = &-\frac{2}{3\Omega}F_{a,b}\delta_{\mu,\nu} \\ &+ \left\{\frac{\pi^2}{2abn_0^{a+b-2}k_F}\sum_{\mathbf{q}\neq 0}[\Delta\tilde{n}_a(\mathbf{q})][\Delta\tilde{n}_b(-\mathbf{q})]\right\} \\ &\times\left(\frac{q_\mu q_\nu}{q^2}-\frac{\delta_{\mu,\nu}}{3}\right)\frac{q}{k_F}\frac{\partial\tilde{w}_{a,b}(q)}{\partial q},\end{aligned} \tag{B9}$$

with $\Delta\tilde{n}_x(\mathbf{q}) = \hat{F}[n^x(\mathbf{r}) - n_0^x(\mathbf{r})]$. While the real space version of $w_{a,b}$ may be found by the inverse Fourier transform,[27] for periodic systems use of the properties of the convolution allow evaluating the free energy as follows:

$$F_{a,b}[n,T] = \int n^a(\mathbf{r},T)\hat{F}^{-1}[\tilde{w}_{a,b}(\mathbf{q},T)\tilde{n}_b(\mathbf{q},T)]\,d\mathbf{r}\ . \tag{B10}$$

Lastly, we give the individual response functions as defined in Eq. (2), needed for evaluating the kernel:

$$\tilde{\chi}_{TF}(T) = -\left(\frac{m_e}{\hbar^2}\right)^{3/2}\frac{1}{2\pi^2}\left(\frac{2}{\beta}\right)^{1/2} I_{-1/2}(\beta\mu_0)\ , \tag{B11}$$

$$\tilde{\chi}_{vW}(\mathbf{q},T) = -\frac{m_e}{\hbar^2}\frac{4k_F^3}{3\pi^2q^2}\ , \tag{B12}$$

$$\tilde{\chi}_{a,b}(\mathbf{q},T) = -\left[2abn_0^{(a+b-2)}\tilde{w}_{a,b}(\mathbf{q},T)\right]^{-1}\ . \tag{B13}$$


[1] F. Lambert, J. Clèrouin, and G. Zèrah, Phys. Rev. E **73**, 016403 (2006).
[2] L. Burakovsky, C. Ticknor, J. D. Kress, L. A. Collins, and F. Lambert, Phys. Rev. E **87**, 023104 (2013).
[3] J.-F. Danel, L. Kazandjian, and G. Zèrah, Phys. Plasmas **15**, 072704 (2008).
[4] F. Perrot, Phys. Rev. A **20**, 586 (1979).
[5] M. Brack, C. Guet, and H.-B. Håkansson, Phys. Rep. **123**, 275 (1985).
[6] V. V. Karasiev, T. Sjostrom, and S. B. Trickey, Phys. Rev. B. **86**, 115101 (2012).
[7] L.-W. Wang and M. P. Teter, Phys. Rev. B **45**, 13196 (1992).
[8] E. Smargiassi and P. A. Madden, Phys. Rev. B **49**, 5220 (1994).
[9] F. Perrot, J. Phys.: Condens. Matter **6**, 431 (1994).
[10] Y. A. Wang, N. Govind, and E. A. Carter, Phys. Rev. B **58**, 13465 (1998).
[11] Y. A. Wang, N. Govind, and E. A. Carter, Phys. Rev. B **60**, 16350 (1999).
[12] C. Huang and E. A. Carter, Phys. Rev. B **81**, 045206 (2010).
[13] J. Xia, C. Huang, I. Shin, and E. A. Carter, J. Chem. Phys. **136**, 084102 (2012).
[14] D. Garcìa-Aldea and J. Alvarellos, Phys. Chem. Chem. Phys. **14**, 1756 (2012).
[15] R. G. Parr and W. Yang, *Density-Functional Theory of Atoms and Molecules* (Oxford, UK, 1989).
[16] B. Holst, R. Redmer, and M. P. Desjarlais, Phys. Rev. B **77**, 184201 (2008).
[17] C. Wang, Y. Long, M.-F. Tian, X.-T. He, and P. Zhang, Phys. Rev. E **87**, 043105 (2013).
[18] T. Sjostrom and J. Dufty, Phys. Rev. B **88**, 115123 (2013).
[19] W. Jones and W. H. Young, J. Phys. C: Solid St. Phys. **4**, 1322 (1971).
[20] Y. A. Wang and E. A. Carter, in *Theoretical Methods in Condensed Phase Chemistry*, edited by S. D. Schwartz, Progress in Theoretical Chemistry and Physics (Kluwer, Dordrecht, 2000), pp. 117–184.
[21] C. H. Hodges, Can. J. Phys. **51**, 1428 (1973).
[22] D. R. Murphy, Phys. Rev. A **24**, 1682 (1981).
[23] G. S. Ho, V. L. Lingères, and E. A. Carter, Comput. Phys. Commun. **179**, 839 (2008).
[24] P. Giannozzi *et al.*, J. Phys. Condens. Matter **21**, 395502 (2009).
[25] J. P. Perdew and A. Zunger, Phys. Rev. B **23**, 5048 (1981).
[26] G. F. Giuliani and G. Vignale, *Quantum Theory of the Electron Gas* (Cambridge University Press, Cambridge, 2005).
[27] Carlos J. Garcìa-Cervera, Commun. Comput. Phys. **2**, 334 (2007).